

Tensor-Force Effects on Nuclear Quadrupole Deformation and $N = 20$ and 28 Magic Numbers

H. Nakada, Y. Suzuki, S. Miyahara

Department of Physics, Graduate School of Science, Chiba University,
Yayoi-cho 1-33, Inage, Chiba 263-8522, Japan

Abstract. Effects of the tensor force on the nuclear quadrupole deformation are investigated, by implementing the Hartree-Fock and the constrained Hartree-Fock calculations assuming the axial symmetry for the proton-deficient $N = 20$ and 28 nuclei. The semi-realistic M3Y-P6 interaction which contains realistic tensor force is applied, and its results are compared with those removing contribution of the tensor force. It is confirmed that the tensor force is repulsive and perturbative. Moreover, the tensor force favors the deformation for the $N = 28$ nuclei, while it favors the sphericity for the $N = 20$ nuclei. These characters are accounted for in terms of the nuclear shell structure for which the ℓs splitting is significant, in addition to the spin-isospin properties of the tensor force. Although these tensor-force effects are partly incorporated in some effective interactions without including the tensor force explicitly, such interactions often lose Z -dependent characters originating from the tensor force, which may be important to describe borderline of the island of inversion.

1 Introduction

One of the goals of the current nuclear structure theory is to understand properties of individual nuclei from the nucleonic interaction. It has been known that the tensor force, which emerges via exchange of pions at the lowest order, is an important ingredient in the nucleonic interaction. However, roles of the tensor force in structure of medium to heavy nuclei have been a hot topic only recently. Experiments using the radioactive beams have revealed Z - or N -dependence of the nuclear shell structure, which is often called *shell evolution*, and it has been recognized that the tensor force plays certain roles in the shell evolution [1–3]. A well-established example of the Z -dependent neutron shell structure is found in the so-called ‘island of inversion (IoI)’, the loss of the $N = 20$ and 28 magicity in the proton-deficient region, as observed in the $E_x(2^+)$ in Figure 1. It has been suggested in many works [4–6] that the IoI occurs via the quadrupole deformation, although other mechanism has not fully been ruled out for some nuclei [7]. An interesting question is whether and how the tensor force contributes to the IoI. The tensor-force effects on the quadrupole deformation have not been investigated sufficiently, while a study using the Skyrme energy density functional

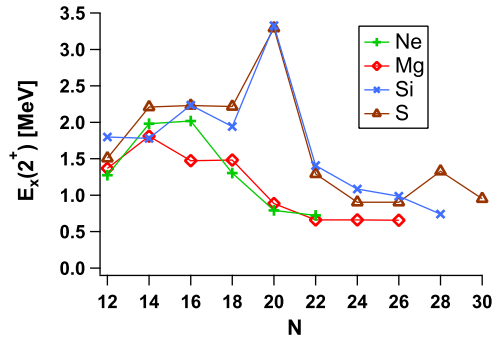


Figure 1. Measured excitation energies of 2_1^+ states around $N = 20$ and 28 . Data are taken from <http://www.nndc.bnl.gov/>.

(EDF) was performed by Bender *et al.* [8] and disclosed some important aspects. However, because the Skyrme EDF is constrained to the quasi-local form, contribution of the tensor force is not well distinguished from that of the central force.

One of the authors (H.N.) has developed semi-realistic nucleonic interactions [9–11], which contain realistic tensor force derived from the G -matrix [12]. Among several parameter-sets of the M3Y-type semi-realistic interactions, M3Y-P6 has been found to predict the shell structure quite reasonably, as exemplified by the magic numbers compatible with available experimental data throughout the nuclear chart with only a few exceptions [3]. It is noted that the realistic tensor force has been important in reproducing Z - and N -dependence of the magic numbers. Because of its realistic nature and reliable prediction on the shell structure, this interaction is useful to investigate the tensor-force effects on the quadrupole deformation, particularly on the onset of the IoI. We shall here present results of the axial Hartree-Fock (HF) calculations using M3Y-P6. While the pairing effects that are lacked in this calculations may influence the deformation, the tensor-force effects become rather clearer in the HF studies rather than in the calculations including the pairing, as will be shown later.

Concerning the IoI, the loss of the $N = 20$ magicity in ^{30}Ne and ^{32}Mg has not been easy to be reproduced within the self-consistent mean-field (MF) calculations [13–15]. It should also be mentioned that, in the prediction of the magic numbers in Ref. [3] which were picked up via quenching of the pair correlations, the loss of the $N = 20$ magicity in ^{32}Mg was not correctly described, as one of the few exceptions mentioned above, while it was reproduced for ^{30}Ne . It is of interest whether and how the quadrupole deformation affects these results.

2 Mean-Field Calculations with Semi-Realistic Interaction

The self-consistent HF calculations are carried out using the non-relativistic effective Hamiltonian. The full Hamiltonian is $H = H_N + V_C - H_{c.m.}$, whose

nuclear part H_N is taken to be isoscalar,

$$H_N = K + V_N; \quad K = \sum_i \frac{\mathbf{P}_i^2}{2M}, \quad V_N = \sum_{i<j} v_{ij}, \quad (1)$$

where i and j represent the indices of individual nucleons. V_C is the Coulomb interaction and $H_{\text{c.m.}} = \mathbf{P}^2/2AM$ is the center-of-mass part, with the total momentum $\mathbf{P} = \sum_i \mathbf{p}_i$ and the mass number $A (= Z + N)$. The effective nucleonic interaction is comprised of two-nucleon central, LS and tensor channels $v^{(C)}$, $v^{(LS)}$, $v^{(TN)}$ and the density-dependent central force $v^{(C\rho)}$. It is stressed that, in M3Y-P6, $v^{(TN)}$ is kept unchanged from the tensor force obtained from the G -matrix [12]. For further details of the interaction, see Ref. [10]. Throughout this study we assume the nuclear state keeps the axial symmetry. With the rotationally invariant Hamiltonian, the rotational symmetry can spontaneously be broken except that along the z -axis.

Numerical calculations are performed by applying the Gaussian expansion method, which was adapted to the deformed MF calculations as discussed in Ref. [16]. As well as searching the energy minima, we have implemented the constrained HF (CHF) calculations. See Ref. [17] for details of the computational procedure. For individual HF (and CHF) state $|\Phi\rangle$, the energy $E = \langle \Phi | H | \Phi \rangle$ and the mass quadrupole moment q_0 ,

$$q_0 = \sqrt{\frac{16\pi}{5}} \langle \Phi | \sum_i r_i'^2 Y_0^{(2)}(\hat{\mathbf{r}}_i) | \Phi \rangle, \quad (2)$$

are computed, where $\mathbf{r}_i' = \mathbf{r}_i - \mathbf{R}$ with $\mathbf{R} = (1/A) \sum_i \mathbf{r}_i$. We then plot the energy curve $E(q_0)$ as below. In order to look into effects of the tensor force, the energy expectation value $E^{(TN)} = \langle \Phi | \sum_{i<j} v_{ij}^{(TN)} | \Phi \rangle$ is computed as well. This is an energy within the first-order perturbation, evaluated at the HF state $|\Phi\rangle$ that obtained in the calculations with the full Hamiltonian. One might think it more desirable to minimize $\langle H - \sum_{i<j} v_{ij}^{(TN)} \rangle$ in investigating tensor-force effects. However, it is not clear what the wave functions minimizing $\langle H - \sum_{i<j} v_{ij}^{(TN)} \rangle$ represent when H itself has been adjusted to basic nuclear properties. Moreover, we have here confirmed that the effects of $v^{(TN)}$ are perturbative in practice, with negligible difference in the energy minima between the perturbative treatment and the minimization.

Another way to see effects of the tensor force is to compare the M3Y-P6 results with those of an interaction well organized without explicit tensor force. For this purpose we employ the Gogny-D1M interaction [18].

3 Application to Proton-Deficient $N = 20$ Nuclei

We present the energy curves $E(q_0)$ of the proton-deficient $N = 20$ nuclei ^{30}Ne , ^{32}Mg and ^{34}Si in Figure 2; $E(q_0)$ and $E(q_0) - E^{(TN)}(q_0)$ with M3Y-P6, and

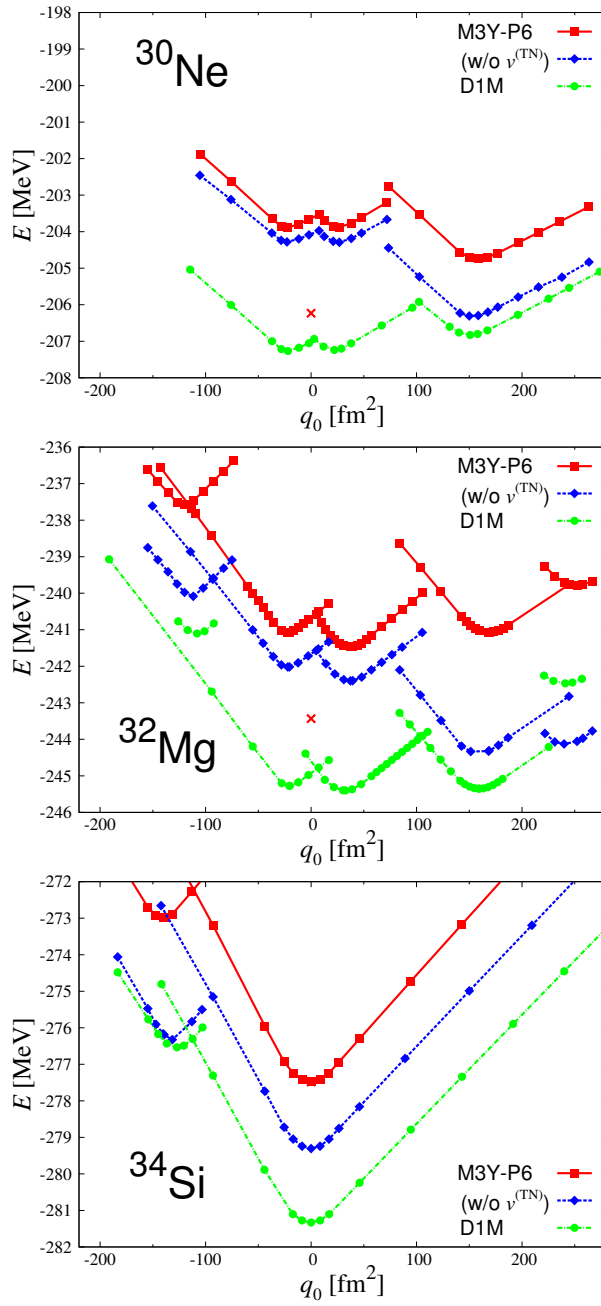


Figure 2. CHF results of $E(q_0)$ (red squares) and $E(q_0) - E^{(TN)}(q_0)$ (blue diamonds) for ³⁰Ne, ³²Mg and ³⁴Si which are obtained with M3Y-P6. For comparison, the energy obtained from the spherical HFB calculation (red cross) and $E(q_0)$ with D1M (green circles) are also plotted. Lines are drawn to guide the eyes. Quote from Ref. [17].

$E(q_0)$ with DIM. The spherical Hartree-Fock-Bogolyubov (HFB) energy with M3Y-P6 is also given for reference.

It is first pointed out that the q_0 values giving the energy minima are very insensitive to the interactions under consideration. In particular, the presence or absence of the tensor force barely influences the q_0 value at each minimum. Together with the close energy between the perturbation and the minimization stated above, this establishes the perturbative nature of the tensor force. However, it is remarked that the amount of the energy contributed by the tensor force significantly depends on the q_0 value, *i.e.*, on the configuration. This finding is an advantage of the HF scheme over, *e.g.*, the HFB approaches. The perturbative nature of the tensor force is obscured via mixing of the configurations, if the variation is carried out including the pairing.

Let us here recall qualitative effects of the tensor force on the spherical orbits [1], originating from its spin-isospin properties. First, it primarily drives proton-neutron correlation. As neutrons occupy a $j'_n = \ell'_n \pm 1/2$ orbit, the tensor force acts attractively on $j_p = \ell_p \mp 1/2$ orbits while repulsively on $j_p = \ell_p \pm 1/2$ orbits, and *vice versa*. If both of the orbits forming an ℓs -partner are fully occupied, contribution of the tensor force vanishes to a good approximation. This is related to the spin saturation and has been proven in general respect in Appendix of Ref. [17]. Quantitatively, the realistic tensor force seems to hold desired strength, as seen in the $p0d_{3/2}$ - $p1s_{1/2}$ inversion from ^{40}Ca to ^{48}Ca [19] and in the low-energy isoscalar $M1$ strength in ^{208}Pb [20].

Owing partly to the perturbative character, these tensor-force effects on the spherical orbits help accounting for effects under deformation. As observed in Figure 2, the tensor force acts repulsively at any q_0 . This should be a general property resulting from the ℓs splitting. Both for protons and neutrons, occupation probability of a valence $j = \ell + 1/2$ orbit is necessarily higher than that of its ℓs partner, at configurations which may form an energy minimum. This makes the tensor force act repulsively, unless negligibly. Therefore, the tensor force tends to favor configuration with spin saturation, at which its repulsive contribution becomes small.

The occupied single-particle (s.p.) levels often provide clear indication to erosion or preservation of the magic numbers. Within the axial HF, each s.p. level has quantum numbers Ω^π , where Ω represents the component of the angular momentum along the symmetry axis and π the parity. In the case of $N = 20$, the highest occupied neutron s.p. level has $\pi = +$ while the lowest unoccupied level has $\pi = -$, if the magicity is preserved. Conversely, when the magicity is lost, there occurs level crossing and one of the $\pi = -$ levels is occupied instead of a $\pi = +$ level. Since the levels having opposite parities do not mix, it is easy to identify from the occupied levels whether the magicity holds or not.

In the $N = 20$ nuclei, the neutron magic number is preserved at the minima in vicinity of $q_0 = 0$. In ^{30}Ne and ^{32}Mg , there are two minima with $q_0 \approx 0$ owing to the partial occupancy of protons on $0d_{5/2}$. The $N = 20$ magicity is hardly broken at these minima. In the configuration keeping the magicity,

the neutron spin degrees-of-freedom (d.o.f.) are almost saturated, since the ℓs partner of any occupied orbit is also fully occupied. Thus the tensor-force effects are small in the configurations which take minima at $q_0 \approx 0$. On the contrary, repulsion from the tensor force comes sizable at the deformed minima, because the neutron state departs from the spin-saturated configuration. Thus the tensor force tends to favor sphericity in the $N = 20$ nuclei, as observed in Figure 2. Note that the contributions of $v^{(TN)}$ are confirmed via the s.p. levels [17].

Comparing the energy curves among the three nuclei, we find that the axial HF approaches with M3Y-P6 predict Z -dependence of shape; from the spherical shape in ^{34}Si to the prolate shape in ^{30}Ne . In ^{32}Mg , the prolate minimum is competing the spherical minima, suggesting the shape coexistence at low energy. Whereas the magicity is kept within the spherical HFB calculation in Ref. [3], the present result indicates that the $N = 20$ magicity could be eroded in ^{32}Mg because of the deformation. These M3Y-P6 results on the proton-deficient $N = 20$ nuclei are qualitatively consistent with experimental data [21–24].

The energy curves with D1M resemble those with M3Y-P6 in ^{32}Mg and ^{34}Si , except for overall shifts of energy. In this respect, the tensor-force effects in M3Y-P6 are more or less incorporated in D1M in an effective manner, though the tensor force is not contained explicitly. However, in ^{30}Ne the prolate minimum lies higher than the spherical minima, unlike the M3Y-P6 results. This seems to imply that the Z -dependence of the energy curve produced by the tensor force is not easy to be followed by the other channels. It is suggested that 0_2^+ (spherical 0^+ state) in ^{30}Ne can be an evidence for the tensor-force effect, whose excitation energy seems to be predicted higher than in ^{32}Mg in the M3Y-P6 result, while similar in the D1M result. Measurement is awaited.

At its ground state, ^{34}Si is predicted to be a doubly-magic nucleus with any of the interaction under consideration, even after taking into account the deformation d.o.f. This suggests that this nucleus remains to be a good candidate of the proton bubble structure [19], in which vacancy of $p1s_{1/2}$ leads to depleted proton density at the nuclear center.

4 Application to Proton-Deficient $N = 28$ Nuclei

In Figure 3, the energy curves are presented for the proton-deficient $N = 28$ nuclei ^{40}Mg , ^{42}Si and ^{44}S .

The repulsive and perturbative characters of the tensor force also hold in the $N = 28$ nuclei, confirming its generality. However, in contrast to $N = 20$, the repulsion from the tensor force is stronger near $q_0 \approx 0$ and diminishes as the deformation develops, in the $N = 28$ nuclei. Origin of this remarkable difference lies in the nature of each magic number: ℓs closure of $N = 20$ and jj closure of $N = 28$. The $N = 28$ magic number results from occupation of the $n0f_{7/2}$ orbit, with its ℓs partner $n0f_{5/2}$ unoccupied. Hence the spherical configuration in the $N = 28$ nuclei is maximally distant from the spin saturation, and suffers the tensor repulsion. As the deformation develops, the system goes

Tensor-Force Effects on Nuclear Quadrupole Deformation

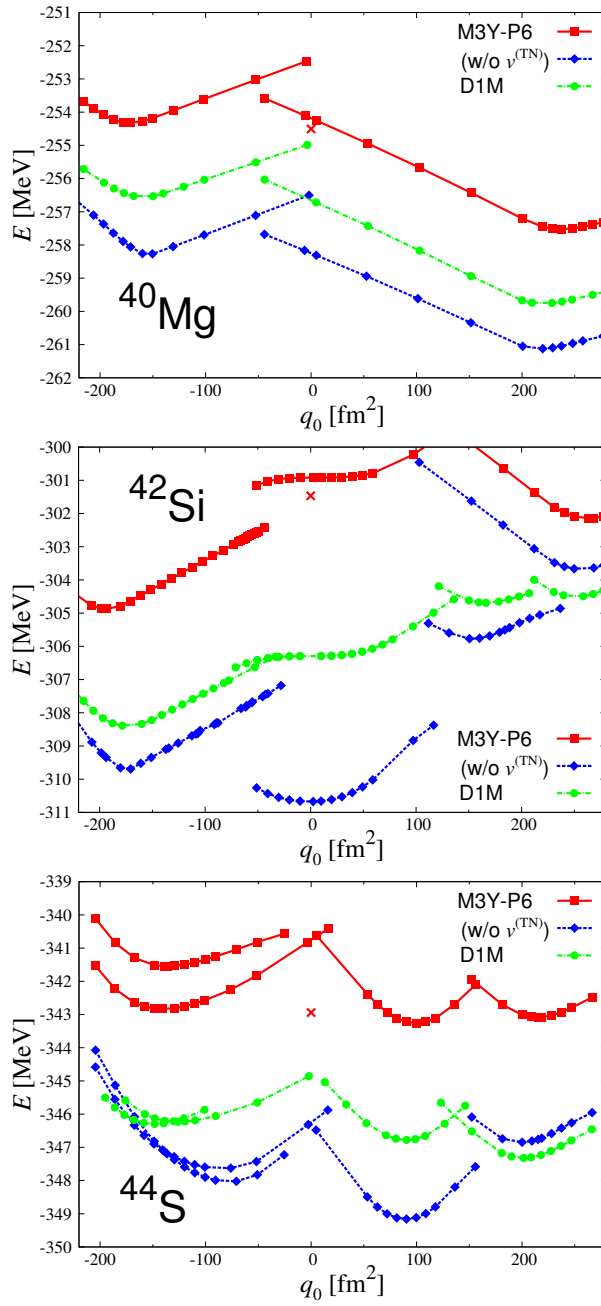


Figure 3. CHF results for ^{40}Mg , ^{42}Si and ^{44}S . See Figure 2 for conventions. Quote from Ref. [17].

toward the spin saturation, by which the tensor repulsion becomes weaker. Thus the tensor force favors deformation in nuclei with the jj -closed magic number as $N = 28$.

In investigating whether the $N = 28$ magic number is preserved or lost, it is again helpful to see properties of the occupied s.p. levels. Unlike the $N = 20$ case, all neutron levels around the Fermi energy have $\pi = -$. Still, when we depart from the spherical limit toward the prolate side, the highest occupied level has $\Omega = 7/2$, which cannot be possessed by adjacent unoccupied levels and therefore hardly mixes with other orbits. This clarifies whether the $N = 28$ magicity is broken or not at the prolate side. In contrast, the highest occupied level has $\Omega^\pi = (1/2)^-$ at the oblate side, which may mix with several unoccupied levels. We need additional care in identifying the magicity at the oblate side. In practice, mixing amplitudes of the spherical s.p. orbitals are used in Ref. [17]. Because the s.p. wave functions are obtained by superposing the spherical bases in the present numerical method, the mixing amplitudes can directly be extracted.

In ^{40}Mg , a prolate configuration gives the lowest minimum, and a oblate configuration the second lowest, even without the tensor force. Similar results were obtained in previous calculations without tensor force [13, 16, 25]. On the other hand, in ^{42}Si the oblate minimum becomes lower than the spherical configuration owing to the tensor force. It is confirmed from the occupied s.p. levels, their mixing amplitudes to be more precise, that the $N = 28$ magicity is eroded in the oblate state. As a part of the tensor-force effects is effectively incorporated, the oblate minimum is the lowest also in the axial HF result with DIM, as in previous studies [13, 14, 25].

In ^{44}S , there are three minima which are close in energy; two prolate minima and an oblate minimum. From the mixing amplitudes of the spherical s.p. components in the occupied s.p. levels, the $N = 28$ magicity is not eroded significantly at the oblate minimum and one of the prolate minima with the weaker deformation. This prediction of the isotonic shape change, the nearly spherical shape in ^{44}S , the oblate in ^{42}Si and the prolate in ^{40}Mg , seems consistent with experiments [26].

5 Summary and Discussion

Tensor-force effects on the nuclear quadrupole deformation have been studied, by implementing the axial HF (including the CHF) calculations in the proton-deficient $N = 20$ and 28 nuclei, ^{30}Ne , ^{32}Mg , ^{34}Si , ^{40}Mg , ^{42}Si and ^{44}S . For the effective nucleonic interaction, the semi-realistic M3Y-P6 interaction is applied, which contains realistic tensor force and has been shown to predict magic numbers compatible with almost all available experimental data. The tensor-force effects are found to be perturbative at the HF level. It should be noted that this simplicity is manifested within the HF scheme, though easily masked by the pairing correlation (in, *e.g.*, the HFB). For low-lying states which could be rele-

vant to the energy curve, the tensor force acts as repulsion, because $j = \ell + 1/2$ orbits have higher occupation probabilities than their ℓs partners for both protons and neutrons. Energy contribution of the tensor force significantly depends on the configuration. As a result, the tensor force favors spherical or deformed shape.

There is a marked difference in the tensor-force effects between $N = 20$ and 28, which locate around the east and west shores of the IoI. In the $N = 20$ nuclei, the repulsion from the tensor force is very weak at the spherical limit because of the spin saturation, while sizable at deformed configurations. In contrast, the tensor repulsion is strongest at the spherical limit in the $N = 28$ nuclei because of the jj closure, which makes the state away from the spin saturation. Thereby the tensor force tends to favor sphericity in $N = 20$ while deformation in $N = 28$. As typically observed in ^{40}Mg , erosion of the magic numbers via deformation, *i.e.*, the IoI, can take place without the tensor force. However, the tensor-force effects are important when several minima are competing, and therefore for the borderline nuclei of the IoI, *e.g.*, ^{32}Mg , ^{30}Ne , ^{42}Si . Although certain part of the tensor-force effects can be incorporated into other channels as viewed in the D1M results, it seems difficult to imitate Z -dependence given by the tensor force completely.

The axial HF results with M3Y-P6 are almost consistent with experimental data, although the pairing and rotational correlations should be taken into account before being conclusive. It may lift the discrepancy at ^{32}Mg in Ref. [3], in which magic numbers are predicted through quenching of the pair correlations. Similar results have been indicated for another region of disagreement, neutron-rich Zr isotopes [27]. Extensive studies including the above mentioned correlations are awaited.

We have clarified perturbative nature of the tensor force, by the HF calculations rather than the HFB, as emphasized already. This seems to justify that the tensor-force effects on the spherical orbits, which were discussed in Ref. [1] at the qualitative level, are straightforwardly transcribed to the deformed nuclei. The effects on the quadrupole deformation observed here are consistent with Ref. [8]. Since we have employed realistic tensor force, the present results are transparent and more reliable, and they can be regarded as confirmation of those in Ref. [8]. Thus the present work must help us comprehend how the tensor force, important ingredient of the nucleonic interaction, affects the nuclear structure, particular on the quadrupole deformation.

References

- [1] T. Otsuka, T. Suzuki, R. Fujimoto, H. Grawe and Y. Akaishi, *Phys. Rev. Lett.* **95** (2005) 232502.
- [2] H. Sagawa and G. Colò, *Prog. Part. Nucl. Phys.* **76** (2014) 76.
- [3] H. Nakada and K. Sugiura, *Prog. Theor. Exp. Phys.* **2014** (2014) 033D02.
- [4] A. Poves and J. Retamosa, *Phys. Lett. B* **184** (1987) 311.

- [5] Y. Utsuno, T. Otsuka, T. Mizusaki and M. Honma, *Phys. Rev. C* **60** (1999) 054315.
- [6] M. Kimura and H. Horiuchi, *Prog. Theor. Phys.* **107** (2002) 33.
- [7] M. Yamagami and N. Van Giai, *Phys. Rev. C* **69** (2004) 034301.
- [8] M. Bender *et al.*, *Phys. Rev. C* **80** (2009) 064302.
- [9] H. Nakada, *Phys. Rev. C* **68** (2003) 014316.
- [10] H. Nakada, *Phys. Rev. C* **87** (2013) 014336.
- [11] H. Nakada and T. Inakura, *Phys. Rev. C* **91** (2015) 021302(R).
- [12] N. Anantaraman, H. Toki and G.F. Bertsch, *Nucl. Phys. A* **398** (1983) 269.
- [13] J. Terasaki, H. Flocard, P.-H. Heenen and P. Bonche, *Nucl. Phys. A* **621** (1997) 706.
- [14] S. Péru, M. Girod and J.F. Berger, *Eur. Phys. J. A* **9** (2000) 35.
- [15] R. Rodoríguez-Guzmán, J.L. Egido and L.M. Robledo, *Nucl. Phys. A* **709** (2002) 201; *Eur. Phys. J. A* **17** (2003) 37.
- [16] H. Nakada, *Nucl. Phys. A* **808** (2008) 47.
- [17] Y. Suzuki, H. Nakada and S. Miyahara, *Phys. Rev. C* **94** (2016) 024343.
- [18] S. Goriely, S. Hilaire, M. Girod and S. Péru, *Phys. Rev. Lett.* **102** (2009) 242501.
- [19] H. Nakada, K. Sugiura and J. Margueron, *Phys. Rev. C* **87** (2013) 067305.
- [20] T. Shizuma *et al.*, *Phys. Rev. C* **78** (2008) 061303(R).
- [21] Y. Yanagisawa *et al.*, *Phys. Lett. B* **566** (2003) 84.
- [22] D. Guillemaud-Mueller *et al.*, *Nucl. Phys. A* **426** (1984) 37.
- [23] R.W. Ibbotson *et al.*, *Phys. Rev. Lett.* **80** (1998) 2081.
- [24] K. Wimmer *et al.*, *Phys. Rev. Lett.* **105** (2010) 252501.
- [25] Z.P. Li *et al.*, *Phys. Rev. C* **84** (2011) 054304.
- [26] H.L. Crawford *et al.*, *Phys. Rev. C* **89** (2014) 041303(R).
- [27] S. Miyahara and H. Nakada, in preparation.